Multipolar electromagnetic fields around neutron stars

Jérôme Pétri
Observatoire astronomique de Strasbourg, Université de Strasbourg, CNRS, UMR 7550, 11 rue de l'université, 67000 Strasbourg, France

2. Braking index for multipoles

The braking index n is deduced from the luminosity L and the rotation Ω

$$n = \frac{\Omega}{L}\frac{dL}{d\Omega} - 1$$

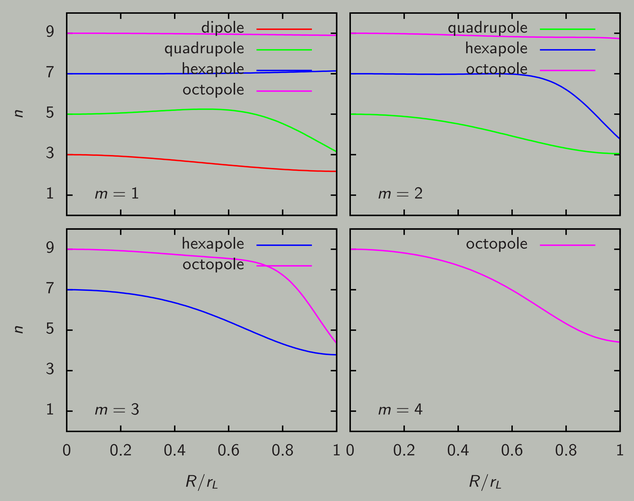

Figure : Braking index according to the ratio R/r_L. The contributions are separated into single components (ℓ, m).

Dipole in agreement with Melatos (1997) from Deutsch (1955) solution.

3. Dipole and quadrupole field lines

The dipole and the quadrupole as illustrative examples of multipolar fields.

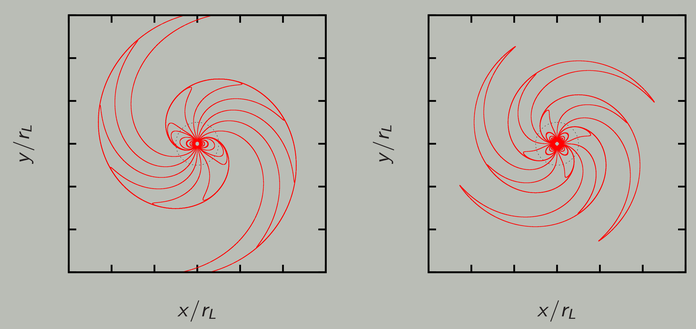

Figure : Geometry of the magnetic field lines in the equatorial plane of an orthogonal point dipole (left) and quadrupole (right).

4. Dipole and quadrupole field estimates

Constraining the magnetic field strength from the Poynting flux.

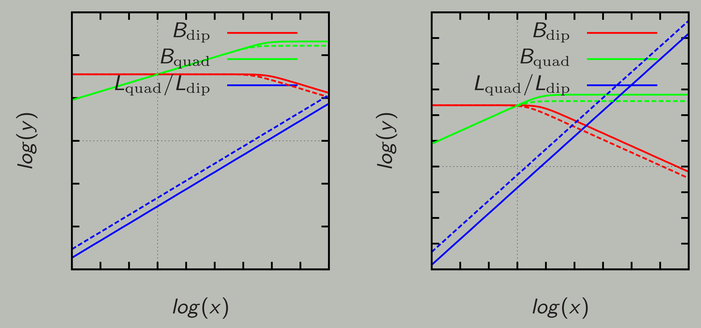

Figure : Ratio of quadrupole to dipole Poynting flux $L_{\rm quad}/L_{\rm dip}$, intensity of dipolar field and quadrupolar field with respect to $x = B_{\rm quad}/B_{\rm dip}$ for normal (left) and millisecond (right) pulsars.

5. Light-curves

Three angles for the set up

- χ for the dipole inclination.
- χ_1, χ_2 for the orientation of the quadrupole.

with respect to the rotation axis.

Rich variety of light-curves with a dipole+quadrupole field with respective weights $w_{\rm d}$ and $w_{\rm q}$ as free parameters.

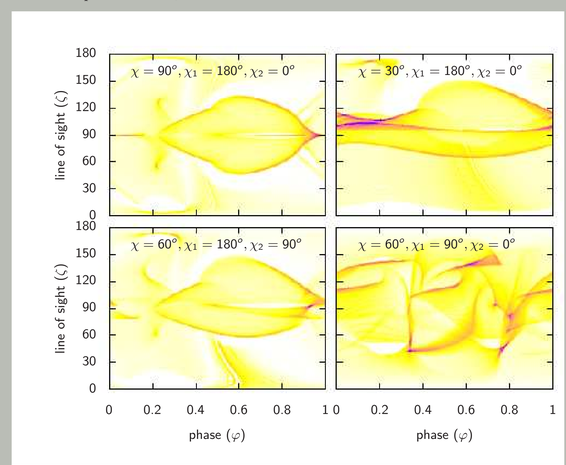

Figure : Phase plots depending on the dipole and quadrupole and the inclination angles $\{\chi, \chi_1, \chi_2\}$ for weights $w_{\rm d} = w_{\rm q} = 1$.

6. Polar cap geometry

Four caps associated to the highest multipole (here the quadrupole).

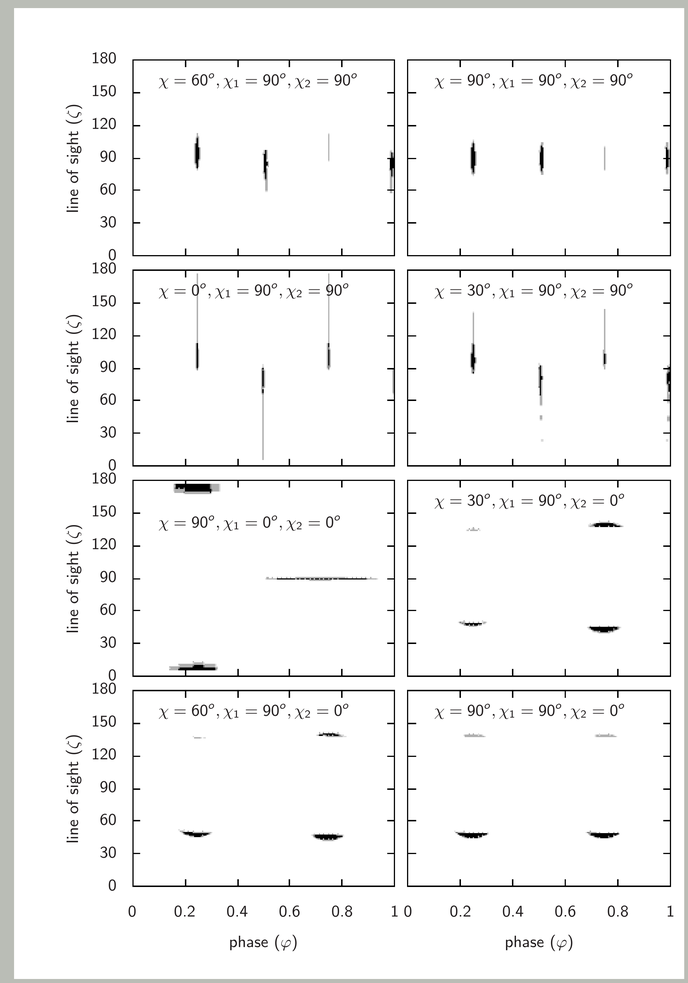

Figure : Geometry of the polar cap for a linear combination of the dipole and quadrupole fields with $R/r_L = 0.1$ and weights $w_{\rm d} = w_{\rm q} = 1$.

Bibliography

Deutsch A. J., 1955, Annales d'Astrophysique, 18, 1
Melatos A., 1997, MNRAS, 288, 1049

jerome.petri@astro.unistra.fr